Available online at www.sciencedirect.com
ScienceDirect
International Journal of Mass Spectrometry 272 (2008) 12–21
International Journal of Mass Spectrometry
www.elsevier.com/locate/ijms

Mass spectrometric study of negative ions extracted from point to plane negative corona discharge in ambient air at atmospheric pressure

Jan D. Skalny [a,*], Juraj Orszagh [a], Nigel J. Mason [b], J. Alan Rees [c], Yolanda Aranda-Gonzalvo [c], Terry D. Whitmore [c]

[a] *Department of Plasma Physics, Comenius University, Mlynska dolina F-2, 84248 Bratislava, Slovakia*
[b] *Department of Physics and Astronomy, Centre of Molecular and Optical Sciences, The Open University, Walton Hall, Milton Keynes MK7 6AA, United Kingdom*
[c] *Plasma & Surface Analysis Division, Hiden Analytical Ltd., 420 Europa Boulevard, Warrington WA5 7UN, United Kingdom*

Received 29 October 2007; received in revised form 13 December 2007; accepted 14 December 2007
Available online 23 December 2007

Abstract

In this paper, we report the detection and mass analysis of negative ions formed in a negative corona discharge using ambient air at atmospheric pressure. Using a mass spectrometer capable of operating at atmospheric pressure with high sensitivity and excellent mass resolution we have detected many anions that were not observable in earlier studies. Practically all the ions detected were in the form of clusters, mostly containing water, although some clusters containing HNO_3 molecules were observed. In contrast to previous reports a relatively high abundance of $O_2^-\cdot(H_2O)_n$ clusters was observed especially when the gap between the two electrodes is small. At larger separations $CO_3^-\cdot(H_2O)_n$, $O_3^-\cdot(H_2O)_n$, $NO_3^-\cdot(H_2O)_n$ and $HCO_3^-\cdot(H_2O)_n$ cluster were detected with yields between 2 and 10%. Previous work has reported negative ion signal with an amu of 125. In contrast to previous suggestions that this represents $OH^-\cdot(H_2O)_6$ we show that it is a cluster of $NO_3^-\cdot HNO_3$. Such results demonstrate conclusively that in any atmospheric pressure discharge most of the ion chemistry involves clusters and therefore models and simulation using unimolecular ions in the description of such discharges are liable to serious misinterpretation.

Keywords: Corona discharge; Mass spectra; Negative ions

1. Introduction

Corona discharges, of either positive or negative polarity, are known to be efficient sources of unipolar ions. However, to date there is relatively little direct information on the mass spectra of ions produced. Knowledge of the composition of such ions is necessary if we are to develop a more detailed understanding of the role of such ions in determining the physical and chemical properties of many devices using corona discharges for example, electrostatic precipitators, air cleaners, ionisers, xerocopy machines and industrial devices used for corona treatment of polymer surfaces. Most of these applications operate corona discharges in ambient air at atmospheric pressure, therefore there is a particular need to characterise ion spectra under such conditions. However it has proven difficult to extract ions from since mass spectrometers operate at pressures typically below 10^{-4} torr such that several regions of differential pumping are required between the source region operating at atmospheric pressure and the mass spectrometer.

There are several studies of corona discharges operating in air over a wide pressure range (0.2–100 kPa) and with different relative humidity (from essentially dry up to air with 100% relative humidity) [1–11]. The pioneering work of Shahin [1] found NO_2^- and O_3^- ions were dominant in a negative corona discharge fed by dry air at *low pressures*. These results were however contrary to those of Gardiner and Cragss [2] who at 1 kPa observed mainly CO_3^- ion with an abundance more than double that of O_3^-, O^- and CO_4^- and only traces of O_2^- ions were detected. These results are in good agreement with our recently published measurements conducted in air at a pressure 5 kPa at low discharge current [3].

* Corresponding author. Tel.: +421 907723010; fax: +421 265425882.
E-mail address: Skalny@fmph.uniba.sk (J.D. Skalny).

1387-3806/$ – see front matter © 2007 Elsevier B.V. All rights reserved.
doi:10.1016/j.ijms.2007.12.012

In Shanin's experiment the abundance of NO_2^- and O_3^- ions in mass spectrum was rapidly reduced with increasing pressure and at atmospheric pressure ions CO_3^- and $CO_3^-{\cdot}H_2O$ were dominant. de Vries et al. [4] and Peyrous et al. [5] in experiments performed at pressures below 300 Torr confirmed the dominant yield of ions CO_3^-, O_3^- and NO_3^- and found that they were usually clustered with water molecules. O_2^-, which could be expected to be dominant in a N_2/O_2 mixture were, in contrast, not observed. Luts [6] explained the absence of O_2^- ions by calculating their lifetime in the discharge to be at most 10 ns while the lifetime of such an ion in clustered form with water molecules is much longer, around 1 s. However, Gravendeel and de Hoog [7] observed single O_2^- ions at pressures up to 600 Torr. Such apparent differences between described experimental results might be due to different water concentrations in the 'dry air'. Gravendeel and de Hoog used synthetic air containing approximately 5 ppm of water vapour and 0.1 ppm of carbon dioxide. The low concentration of carbon dioxide is therefore the most likely reason for the O_3^- being dominant instead of CO_3^- in their experiments.

A second factor that may influence the measured anion spectra of ions is the concentration of products generated in the corona discharge. There are principally two types of experiments analysing mass spectra of ions produced by corona discharges in air. In the first scenario air is continuously flowing through the discharge gap and thence the chemical products, especially ozone and nitrogen oxides may be efficiently removed from the discharge. The concentration of chemical products within the discharge is then determined by flow rate through the discharge and the energy density loaded into discharge. In the second scenario experiments are performed in so called flow-stopped or 'static' regime with no gas flow through the discharge. Under these conditions chemical products are accumulated in the discharge gap and their concentration is affected by time and by energy density loaded into the discharge.

Ross and Bell [8] explored the differences in these two regimes using an IMS (ion mobility spectrometer) to analyse ions produced in a negative corona discharge in flowing air using a 'point to plane electrode system'. In the first mode the gas flow was oriented down the axis of the reactor in the same direction as the velocity of ions drifting from the point to plane. The concentration of CO_3^- and O_3^- ions was observed to increase with the flow rate while the concentration of NO_3^- was reduced, no O_2^- ions were observed and the concentration of CO_4^- was very low. In contrast when the air flow was oriented against the ion flow all the chemical compounds generated at the tip of the point electrode were removed from the drift region and high concentrations of O_2^- were detected. Moreover the concentration of CO_4^- increased linearly with flow rate. In contrast concentrations of CO_3^-, O_3^- and NO_3^- were reduced dramatically (almost to zero) with increasing flow rate. Thus there is clear evidence that the ion–molecule reactions in the drift region of the discharge determine the composition of the ions produced by corona discharges.

Further evidence for the important role of chemical compounds formed in the discharge gap is presented in our recent paper [9]. The mass spectra of ions extracted from negative corona in 30 kPa generated in ambient air obtained in flow-stopped regime were analysed. It was evident from the measured time dependence of the yield of individual ions that, due to the increase in the concentrations of nitrogen oxides and ozone in the discharge gap, the yield of CO_3^- ion and its water clusters decreases in time, while the yield of stable ions $NO_3^-{\cdot}(H_2O)_n$ increases. Finally the experiments of Nagato et al. [10] performed in flowing humid air containing traces of SO_2 have shown that, even with concentrations of SO_2 smaller than 4 ppm, the spectrum of ions is dramatically changed compared to 'pure air'. SO_2^-, SO_3^-, SO_4^- and HSO_4^- dominate the measured spectra and even clusters containing H_2SO_4 molecules were observed.

In recent experiments Nagato et al. [11] showed that an important parameter influencing the recorded mass spectra is the drift time of ions. Combining their corona discharge reactor with a mass spectrometer and time of flight spectrometer they showed that if the drift time of ions was greater than 10 μs CO_3^- ions and its water clusters disappeared from the spectra and the concentration of $NO_3^-{\cdot}(H_2O)_n$ rapidly increased. Moreover at such large flight times $HCO_3^-{\cdot}HNO_3$ and $NO_3^-{\cdot}NO_3$ anions were detected with large abundances.

In the present paper we present the spectra of anions produced in a negative corona discharge fed by ambient air under static conditions of a static recorded using the Hiden HPR60 MBMS spectrometer operating at atmospheric pressure at its inlet. The effect of distance between point and plane electrodes on the composition of mass spectra of ions extracted through the orifice in plane electrode is presented.

2. Experimental apparatus

The apparatus used in these experiments is shown schematically in Fig. 1. A simple point to plane corona discharge was formed by placing a pointed stainless steel needle in close proximity to the wall of a vacuum chamber (the wall acting as a planar electrode). A small orifice (diameter of 0.1 mm) in the wall of the vacuum chamber allowed the products of the discharge to

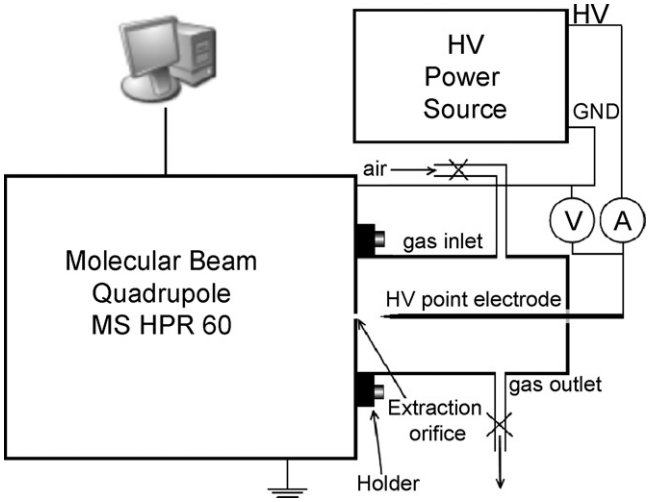

Fig. 1. A schematic diagram of the experimental apparatus used in the present experiments.

enter a Hiden Molecular Beam Quadrupole MS HPR60. The discharge region was surrounded by a plastic chamber forming a volume of approximately 300 cm^3 into which the feed gas for the discharge could be injected. Experiments were performed using the ambient air of the laboratory at atmospheric pressure and ambient temperature, 20 °C. The point electrode was powered by a Spellman HV source whose output was measured using a HV probe combined with a digital multi-meter. The discharge current was measured using a microampmeter.

3. Experimental results and discussion

All experiments were performed in a static regime with air being introduced into the discharge chamber and then the discharge volume was sealed. Mass spectra were recorded after allowing a suitable time for the discharge to stabilise. Stable conditions in the discharge were assumed when the ozone yield reached a constant value.

The relative yield Y_r of ions having a mass per charge smaller than 160 was calculated from the measured absolute yield of ions i-type in spectra Y_i by the formula

$$Y_r = \frac{Y_i}{\sum_i Y_i} \times 100\,(\%)$$

Typical mass spectra obtained at two different separations between the electrodes but with the same current (50 μA) are shown in Figs. 2 and 3. It is evident that the separation distance between the electrodes dramatically changes the mass spectra. The abundances of ions at $Z<60$ and $Z>160$ were negligible and are therefore not displayed. Practically all the negative ions detected were in the form of clusters, mostly containing water, although some clusters containing HNO_3 and O_2 or even combinations of such molecules were also observed.

The transport time of any of these ions in the discharge can be calculated using the formula

$$\int_0^{\tau} \mathrm{d}t = \int_{r_0}^{L} \frac{1}{E(x)\mu}\mathrm{d}x \tag{1}$$

where τ is transport time, L the distance between electrodes, r_0 tip radius of point electrode, $E(x)$ is the intensity of electric field along the discharge gap, μ the mobility of ions and x is the distance between point and plane electrodes. If we use the approximate formula given by Lamma and Gallo [12] for $E(x)$ then (1) can be expressed as follows

$$\tau = \frac{1}{4\mu U} \ln \frac{4L}{r_0} L^2 \tag{2}$$

where U is the voltage on electrodes. The tip radius was determined, using a scanning electron microscope, to be 0.02 mm. The length L was varied from 6 to 18 mm and voltage U between 4.6 and 15 kV. If we use the mean value of ion mobility of 2 $cm^2/(V\,s)$ then τ varies from 0.06 ms up to 0.2 ms over this range of U.

The characteristic time t_{char} of any individual ion process

$$A^- + B \rightarrow A + B^- \tag{3}$$

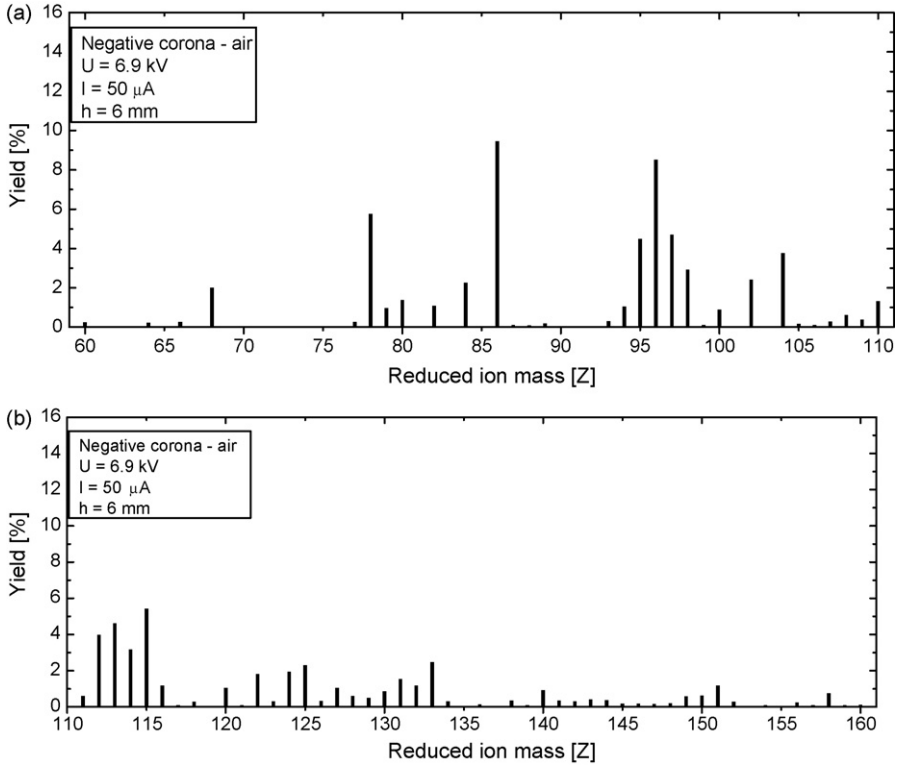

Fig. 2. (a and b) Complete mass spectrum of negative ions extracted from the discharge operated with electrode separation of $h = 6$ mm.

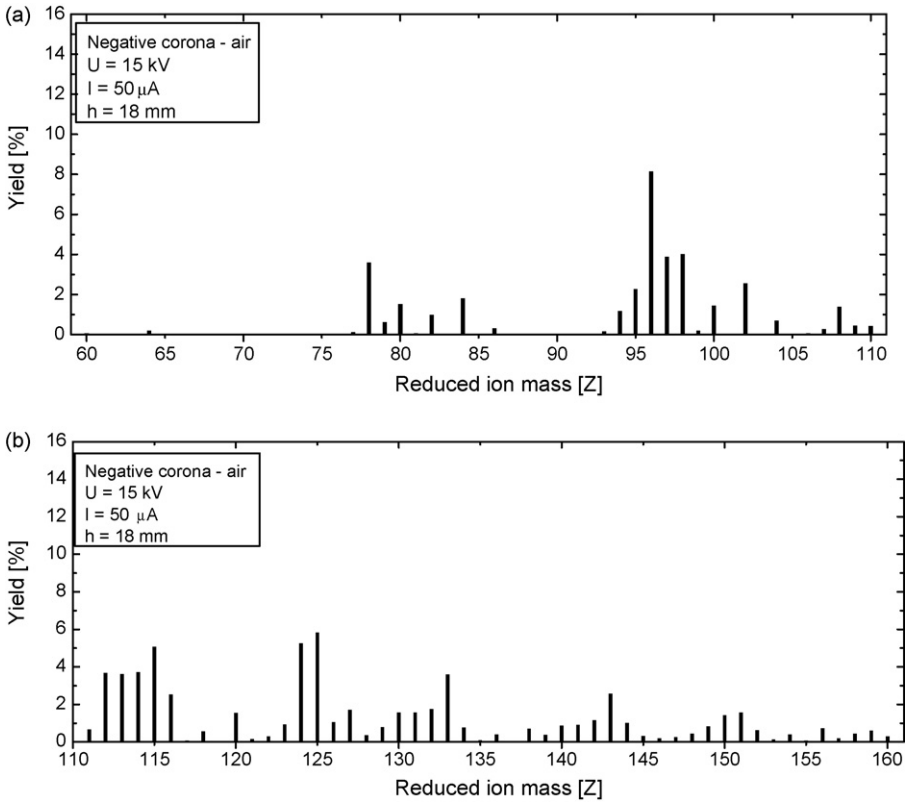

Fig. 3. (a and b) Complete mass spectrum of negative ions extracted from the discharge operated with electrode separation of $h = 18$ mm.

can then be written as

$$t_{\text{char}} = \frac{1}{k[\text{B}]} \tag{4}$$

If t_{char} is shorter than the transport time τ then ion/molecule reaction (3) will determine the final anion mass spectrum.

We will now discuss the formation and behavior of each of the major anions observed in the spectra.

In any atmospheric pressure discharge the negative ions with the largest concentrations are expected to be formed from the most electronegative species which, in the case of ambient air, is molecular oxygen. Thus we might expect to observe both O^- and $O_2{}^-$ in our mass spectra formed by dissociative electron attachment and three body electron attachment

$$\text{e} + \text{O}_2 \rightarrow \text{O}^- + \text{O} \qquad k_5 = f(E/N) \quad [13] \tag{5}$$

$$\text{e} + \text{O}_2 + \text{M} \rightarrow \text{O}_2{}^- + \text{M} \qquad k_6 = f(E/N) \quad [13] \tag{6}$$

The formation of O^- is confined to a small volume around the tip of point electrode the so called 'ionisation' or 'glow region' while $O_2{}^-$ is formed predominately in drift region of the discharge where the reduced electric field is low. However, none of our spectra revealed any such anions but instead showed large numbers of cluster ions, in particular ions cluster with water molecules. Ambient air always contains water its concentration being defined by its 'humidity', thus although present in small concentrations it appears it is the amount of water in the discharge that drives much of the physics and chemistry. Furthermore the appearance of $CO_3{}^-$, $O_3{}^-$, $NO_2{}^-$, $NO_3{}^-$ and $HCO_3{}^-$ reveals further complex chemistry in the discharge that requires discussion.

3.1. O^- chemistry and the formation of $CO_3{}^-$ and its associated solvated clusters

In the presence of carbon dioxide O^- anions are rapidly converted into $CO_3{}^-$ anions

$$\text{O}^- + \text{CO}_2 + \text{M} \rightarrow \text{CO}_3{}^- + \text{M}$$
$$k_7 = 1 \times 10^{-29}\,\text{cm}^6/\text{s} \quad [14] \tag{7}$$

Due to its high electron affinity the $CO_3{}^-$ anion is stable and hence may create water clusters efficiently through the process

$$\text{CO}_3{}^- + \text{H}_2\text{O} + \text{M} \rightarrow \text{CO}_3{}^-\cdot\text{H}_2\text{O} + \text{M}$$
$$k_8 = 1 \times 10^{-28}\,\text{cm}^6/\text{s} \quad [7] \tag{8}$$

which is followed by a series of secondary clustering reactions [15] leading to the formation of still larger clusters $CO_3{}^-\cdot(H_2O)_n$ e.g.,

$$\text{CO}_3{}^-\cdot\text{H}_2\text{O} + \text{H}_2\text{O} + \text{M} \rightarrow \text{CO}_3{}^-\cdot(\text{H}_2\text{O})_2 + \text{M} \tag{9}$$

The rate constant of this step and further steps in which clusters $CO_3{}^-\cdot(H_2O)_n$ are formed is unknown but is likely to be of the order of $10^{-28}\,\text{cm}^6/\text{s}$. Such a high rate constant can be surmised from the high abundance of such ions in all the

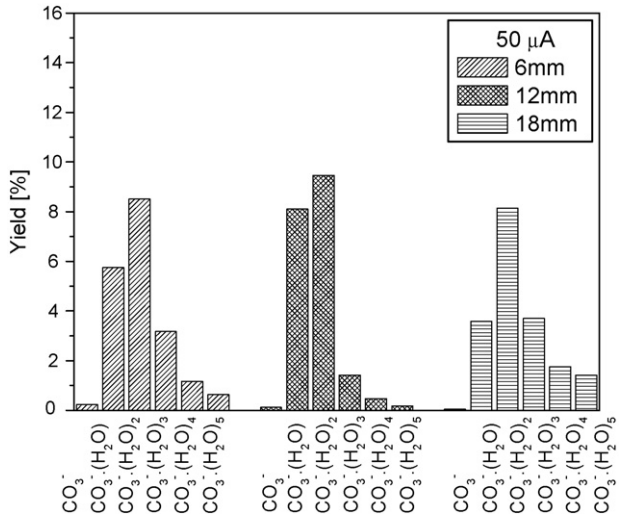

Fig. 4. The relative abundances of $CO_3^-\cdot(H_2O)_n$ at three electrodes distances.

mass spectra recorded (Fig. 4). A slight decrease in the yield of $CO_3^-(H_2O)_n$ anions is observed with increasing electrode separation while at low discharge currents the relative abundance of $CO_3^-\cdot(H_2O)_n$ appears to increase. It must be noted, however, that the abundance of the $CO_3^-(H_2O)_n$ is also influenced by the reverse reaction of (9) and some further experiments with regulated humidity are required.

This later effect may be ascribed to a decrease in the production of ozone and nitrogen oxides at low discharge currents, compounds that can lead to the removal of $CO_3^-\cdot(H_2O)_n$ anions.

The increase in relative abundance of clusters $CO_3^-\cdot(H_2O)_n$ at low current can also be a consequence of changes in the reduced electric field *E*/*N* (E—electric field, N—concentration of particles in reactor, in our case 2.68×10^{19} particles/cm^3). The discharge current decreases as the voltage on electrodes decreases. This is accompanied by a decrease of *E*/*N* in the drift region, especially at plane electrode. Moreover, increasing distance between electrodes also leads to a reduction of *E*/*N* and consequently an increase in the abundance of clusters.

The CO_3^- anion and its water clusters may also form NO_2^- ions by reactions with nitrogen oxides

$$CO_3^- + NO_2 \rightarrow CO_2 + NO_3^-$$
$$k_{10} = 2\times10^{-10}\,\mathrm{cm^3/s} \quad [7] \tag{10}$$

$$CO_3^-\cdot(H_2O)_n + NO_2 \rightarrow NO_3^-\cdot(H_2O)_n + CO_2$$
$$k_{11} = 1.5\times10^{-10}\,\mathrm{cm^3/s} \quad [7] \tag{11}$$

The last process is the one most likely to be responsible for the increased concentration of $NO_3^-\cdot(H_2O)_n$ clusters observed with increasing distance between the point and plane electrodes.

Clusters of $CO_3^-\cdot(O_2)_n$ were also present in spectrum. It was however not possible to analyse these spectra since $CO_3^-\cdot O_2$ has a unique mass in the recorded spectrum the other $CO_3^-\cdot(O_2)_n$ ($n>2$) anions have the same mass as other anionic species, e.g., $CO_3^-\cdot(O_2)_2$ with $HCO_3^-\cdot HNO_3$ and $CO_3^-\cdot(O_2)_3$ with $O_3^-\cdot(H_2O)_6$.

A third type of cluster which might be observed were clusters of $CO_3^-\cdot HNO_3$ but these were only observed at abundances lower than 1%. It must be noted that this ion is commonly observed in atmospheric plasma chemistry [16,17] but surprisingly the abundance in the discharge gap is low.

3.2. O_2^- ion chemistry and cluster formation

O_2^- anions, formed by direct electron attachment (2) are stable at high pressure and react readily with water in a series of step by step processes the first of which is

$$O_2^- + (H_2O)_n + M \rightarrow O_2^-\cdot(H_2O)_n + M$$
$$k_{12} = 2\times10^{-28}\,\mathrm{cm^6/s} \quad [7] \tag{12}$$

However, it is evident from Fig. 5 that these water clusters are greatly reduced as the distance between the point and plane electrodes is increased. The abundances of $O_2^-\cdot(H_2O)_n$ ions were even higher at low current densities when the electric field is low in the drift region.

There are several reactions by which O_2^- anions may be removed from the discharge, Ross and Bell [8]. The fastest process is conversion of O_2^- to O_3^-

$$O_2^- + O_3 \rightarrow O_3^- + O_2 \qquad k_{13} = 3\times10^{-10}\,\mathrm{cm^3/s} \quad [13] \tag{13}$$

which has a characteristic time of 5 ns in an atmospheric pressure discharge. Therefore in the presence of ozone the O_2^- ions are efficiently removed by (13). The longer the drift time the lower the yield of O_2^- (and its clusters) as observed in Fig. 5. Similarly O_2^- reacts with any NO_2 present in the discharge gap through

$$O_2^- + NO_2 \rightarrow NO_2^- + O_2 \qquad k_{14} = 2\times10^{-9}\,\mathrm{cm^3/s} \quad [7] \tag{14}$$

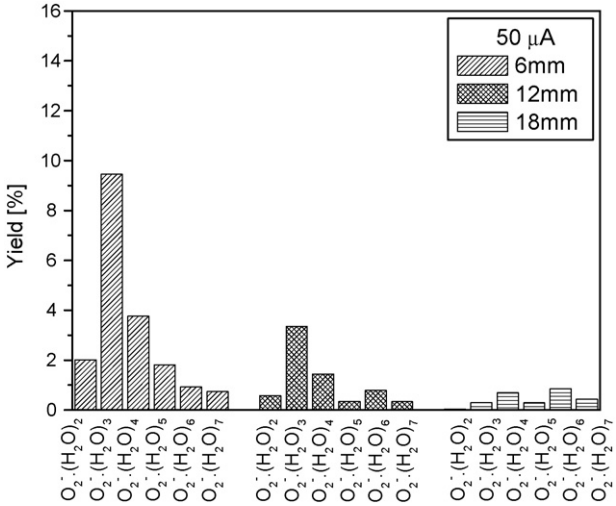

Fig. 5. The relative abundances of $O_2^-\cdot(H_2O)_n$ recorded for three different electrode separations.

with a characteristic time of 21 ns. NO_2^- ions may then cluster with water through the reaction

$$O_2^-\cdot(H_2O)_n + NO_2 \rightarrow NO_2^-\cdot(H_2O)_{n-1} + O_2 + H_2O$$
$$k_{15} = 9\times10^{-10}\,cm^3/s \quad [7] \qquad (15)$$

The last process (15) is most probably responsible for the observed increase in the concentration of $NO_2^-\cdot(H_2O)_n$ clusters at larger electrode separation and may provide evidence for the importance of the transport of such species within the discharge.

O_2^- ions can also be converted into O_4^- ions through a very rapid reaction

$$O_2^- + O_2 \rightarrow O_4^- \qquad k_{16} = 2\times10^{-9}\,cm^3/s \quad [7] \qquad (16)$$

O_4^- ions are $O_2^-\cdot O_2$ clusters, which are very weakly bounded and thus are unstable in high electric fields. $O_2^-\cdot O_2$ clusters (mass 64) have the same mass as $NO_2^-\cdot H_2O$ clusters hence it is not easy to ascribe the signal at mass 64 to any one ion. However, the ion signal with mass 64 increases with discharge current and thence with increasing electric field which would suggest that it is unlikely to be due to the unstable $O_2^-\cdot O_2$ cluster and therefore we assign such signal to $NO_2^-\cdot H_2O$ cluster.

Not only water clusters were observed, a relatively strong signal was observed at mass 95 and is ascribed to the formation of $O_2^-\cdot HNO_3$ clusters. The yield of this ion was seen to decrease with increasing distance of electrodes. In contrast to water clusters there were few heavier clusters with yields of $O_2^-\cdot(HNO_3)_2$ below 1%.

3.3. O_3^- ion and its clusters

Ozone is a major chemical product of discharges in any oxygen rich gas. If the concentration of ozone in the discharge gap is low, the three body process

$$O^- + O_2 + M \rightarrow O_3^- + M$$
$$k_{17} = 3.3\times10^{-31}\,cm^6/s \quad [13] \qquad (17)$$

is the only potential source of O_3^- ions. However, O_3^- can also be formed in the charge transfer process

$$O^- + O_3 \rightarrow O_3^- + O \qquad k_{18} = 5.3\times10^{-10}\,cm^3/s \quad [13] \qquad (18)$$

This process starts to be dominant if

$$[O_3] \geq \frac{0.2[M]^2 k_{17}}{k_{18}} \qquad (19)$$

At atmospheric pressure $M = 2.68\times10^{19}$ molecule cm^{-3}, it therefore follows that at atmospheric pressure ozone concentration $[O_3]$ must be higher than 3300 ppm if process (18) is to be the main process by which O_3^- is produced. This value is unlikely in our experiments; hence the dominant primary source of negative ozone ions is the three body process (17).

Another channel for formation of O_3^- ions is the ion reaction (13). This in turn will only be the dominant source of ozone anions if

$$[O_3] \geq \frac{k_{17}0.2[M^2]}{k_{13}} \qquad (20)$$

It must be noted however that condition (20) is valid only if concentrations $[O^-]$ and $[O_2^-]$ are comparable. At atmospheric pressure this condition is only fulfilled when ozone concentrations exceed 5800 ppm, which is not a realistic value in our experiment. Hence once again we conclude that the main source of the O_3^- ions in our reactor will be due to the three body process (17). The observed decrease in $O_3^-\cdot(H_2O)_n$ yield as the discharge current increases supports this hypothesis. If either processes (13) and (18) were dominant the yield of $O_3^-\cdot(H_2O)_n$ clusters would increase with increasing discharge current since ozone yields increase as the discharge current increases. However, just the opposite effect was observed (compare Figs. 6 and 7). This is due to a decrease in rate constant of process (17) with increasing discharge cur-

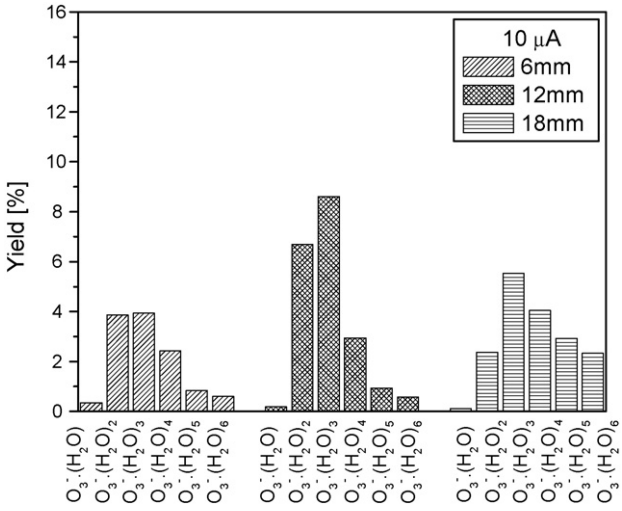

Fig. 6. The relative abundances of $O_3^-\cdot(H_2O)_n$ at three electrodes distances and low discharge current.

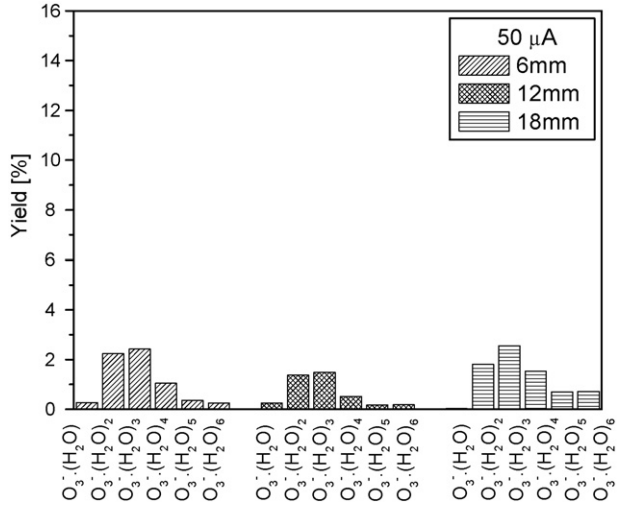

Fig. 7. The relative abundances of $O_3^-\cdot(H_2O)_n$ at three electrodes distances and the highest discharge current.

rent and hence increasing electric field in the discharge gap [13].

In fact no O_3^- monomers were observed in any of our mass spectra but relatively high concentrations of ozone/water anions clusters were detected (Figs. 6 and 7). $O_3^-\cdot(H_2O)_n$ clusters are formed in consecutive reactions

$$O_3^-\cdot(H_2O)_n + H_2O + M \rightarrow O_3^-\cdot(H_2O)_{n+1} + M$$
$$n = 0, 1, 2 \ldots k_{21} \approx 1 \times 10^{-28}\,\mathrm{cm}^6/\mathrm{s} \quad [7] \qquad (21)$$

In addition to cluster formation there are several other processes that can result in the removal of O_3^- anions from the discharge [13] but only four of them are important under corona discharge conditions

$$O_3^- + CO_2 \rightarrow CO_3^- + O_2$$
$$k_{22} = 6 \times 10^{-10}\,\mathrm{cm}^3/\mathrm{s} \quad [14] \qquad (22)$$

$$O_3^- + M \rightarrow O_3 + M + e$$
$$k_{23} = 2.3 \times 10^{-11}\,\mathrm{cm}^3/\mathrm{s} \quad [13] \qquad (23)$$

$$O_3^- + NO_2 \rightarrow NO_3^- + O_2$$
$$k_{24} = 1 \times 10^{-11}\,\mathrm{cm}^3/\mathrm{s} \quad [14] \qquad (24)$$

$$O_3^- + NO_2 \rightarrow NO_2^- + O_3$$
$$k_{25} = 7 \times 10^{-10}\,\mathrm{cm}^3/\mathrm{s} \quad [7] \qquad (25)$$

The efficiency of concurrent processes (24) and (25) as a function of gas temperature has been studied by Arnold et al. [18] and [19]. The rate constant found for both processes is substantially smaller (3×10^{-12} cm^3/s at $T = 300$ K) than the older data k_{24} and k_{25}.

Among listed reactions (22)–(25) the shortest characteristic time (only 16 ns) is for the detachment process (23) providing a source of additional free electrons in the drift region.

Clusters of $O_3^-\cdot(HNO_3)_n$ and $O_3^-\cdot(O_2)_n$ clusters were also observed in the mass spectrum. But their abundances were below 1%.

3.4. NO_2^- ion and its clusters

The abundance of $NO_2^-\cdot(H_2O)_n$ clusters was found to be low but increased with increasing distance between the electrodes through processes (14) and (15) (Fig. 8). No $NO_2^{\bullet -}$ parent ions were detectable.

3.5. NO_3^- ions and its clusters

No NO_3^- ions were observed in our mass spectra. All such ions were found in the form of water clusters $NO_3^-\cdot(H_2O)_n$. Increasing the distance between electrodes increased the yield of such clusters in the spectra (Fig. 9) especially at high currents.

NO_3^- ions will be generated through process (10) and are quickly converted to water clusters, or, and this is more probable, the clusters are formed directly by process (11). A complete analysis of the formation of such anions is complicated by the lack of data for clustering of ions $NO_3^{\bullet -}$ with water molecules. However, due to their high electron affinity NO_3^- ions are stable hence one can suppose that the cluster forms are also stable.

There are only two reactions by which NO_3^- anions are destroyed in the discharge [7]

$$NO_3^- + O \rightarrow \text{products} \quad k_{26} = 1 \times 10^{-11}\,\mathrm{cm}^3/\mathrm{s} \quad [7] \qquad (26)$$

$$NO_3^- + NO \rightarrow NO_2^- + NO_2$$
$$k_{27} = 1 \times 10^{-12}\,\mathrm{cm}^3/\mathrm{s} \quad [7] \qquad (27)$$

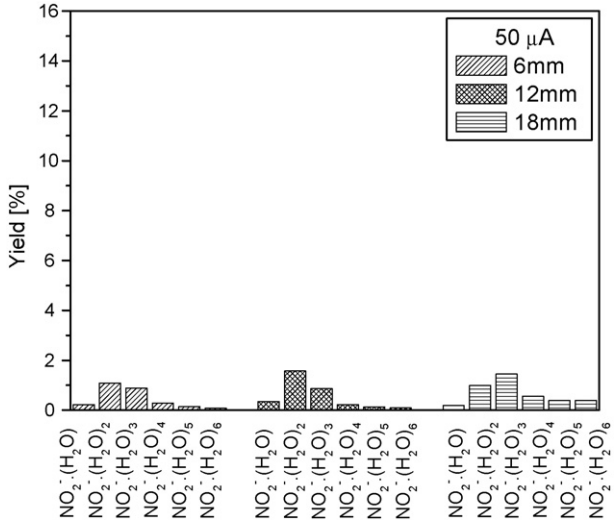

Fig. 8. The relative abundances of $NO_2^-\cdot(H_2O)_n$ at three electrodes distances and the highest discharge current.

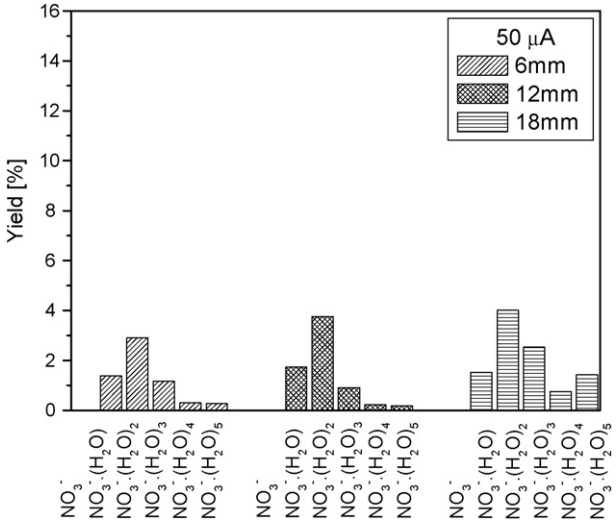

Fig. 9. The relative abundances of $NO_3^-\cdot(H_2O)_n$ at three electrodes distances and the highest discharge current.

The values of the rate constants k_{26} and k_{27} are the upper limits of those reactions. The first reaction is very inefficient because the concentration of atomic oxygen is only high enough in the glow region where practically no NO_3^- ions are created. The characteristic time for the second reaction is more than 10 ms making it equally unlikely.

Clusters of $NO_3^-\cdot HNO_3$ were also observed in the experiment (mass 125) with relatively high abundances, increasing from 2.3% at electrode separation of 6 mm to 5.8% at distance of 18 mm. This observation is in agreement with earlier work by Nagato et al. [11] who found after transport times of 10 ms that this ion was one of three dominant ions observed in their spectra. It must be noted however that the mass 125 corresponds also to the ion $HCO_3^-\cdot(O_2)_2$ while Gravendeel and de Hoog [7] ascribed this mass to the $OH^-\cdot(H_2O)_6$ cluster ion, although as we will discuss later we do not believe this interpretation to be valid.

Mass peaks that can be ascribed to $NO_3^-\cdot(O_2)_n$ clusters were also observed (masses 94, 126 and 158) but none had yields in excess of 1%.

3.6. OH^- ion and its clusters

No OH^- ions were observed in our mass spectra but $OH^-\cdot(H_2O)_n$ clusters up to $n=7$ were readily detected (see Figs. 10 and 11) in agreement with Nagato et al. [11] and Gravendeel and de Hoog [7]. Such anions are formed through multi-step clustering with

$$OH^-\cdot(H_2O)_n + H_2O + M \rightarrow OH^-\cdot(H_2O)_{n+1} + M$$
$$n = 0, 1, 2\ldots \quad k_{28} \approx 5\times10^{-28}\,\mathrm{cm^6/s} \quad [7] \qquad (28)$$

The yield of OH^- increases nearly exponentially with air pressure in range of 500–1000 mbar. This suggests that formation of OH^- anions is a three body process. This is however, in contrast with the suggestion by Nagato et al. [11] who proposed

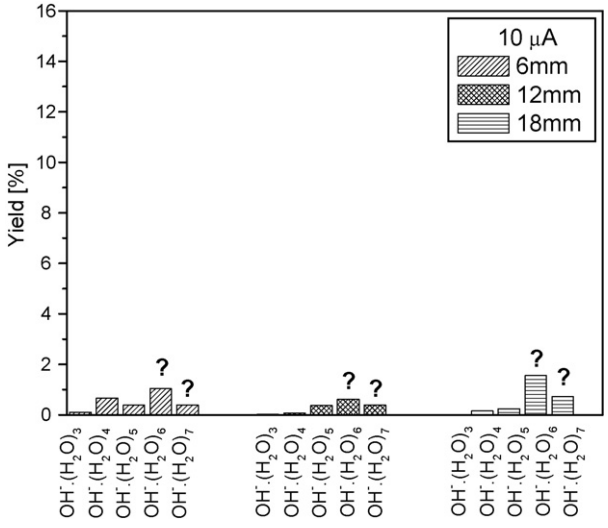

Fig. 10. The relative abundances of $OH^-\cdot(H_2O)_n$ at three electrodes distances and low discharge current.

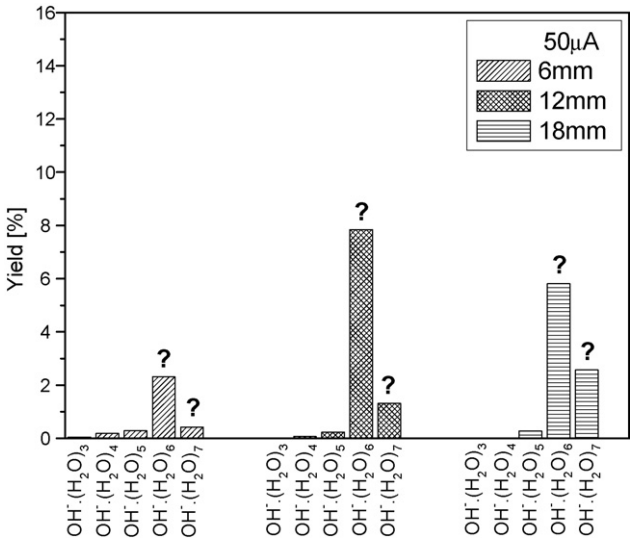

Fig. 11. The relative abundances of $OH^-\cdot(H_2O)_n$ at three electrodes distances and the highest discharge current.

such ions to be formed by

$$O^- + H_2O \rightarrow OH^- + OH \quad k_{29} = 6\times10^{-13}\,\mathrm{cm^3/s} \quad [11] \qquad (29)$$

The characteristic time for this process for a relative humidity of 50% and a $T=300$ K is 4.3 μs which is substantially longer time than any other reactions discussed so far. Therefore we can conclude that such a slow process as (29) cannot be the major source of OH^- ions. According to Gravendeel and de Hoog [7] the OH^- anions are formed by dissociative electron attachment to water molecules

$$e + H_2O \rightarrow OH^- + H \qquad k_{30} = f(E/N) \qquad (30)$$

However, such hypothesis about the origin of OH^- ion and its clusters cannot explain the existence of such ions in our spectra. Moreover the considerable increase in abundance of such ions with air pressure observed by Gravendeel and de Hoog [7] leads to propose another mechanism of formation of $OH^-\cdot(H_2O)_n$ clusters. In our opinion the primary ion O^- reacts in three body process with water

$$O^- + H_2O + O_2 \rightarrow O^-\cdot H_2O + O_2$$
$$k_{31} = 1.3\times10^{-28}\,\mathrm{cm^6/s} \quad [20] \qquad (31)$$

The reaction time is very short of 4.7 ns at relative humidity 50% and $T=300$ K which makes this reaction highly probable. In the second step the $O^-.H_2O$ clusters are converted in bimolecular processes

$$O^-\cdot H_2O + H_2O \rightarrow OH^-\cdot H_2O + OH$$
$$k_{32} > 1\times10^{-11}\,\mathrm{cm^3/s} \quad [20] \qquad (32)$$

$$O^-\cdot H_2O + H_2O \rightarrow O_3^- + H_2O$$
$$k_{33} > 1\times10^{-11}\,\mathrm{cm^3/s} \quad [20] \qquad (33)$$

While the second process is source of O_3^- ions, process (33) is the source of $OH^-\cdot H_2O$ clusters. These are clustered with water molecules and form the $OH^-\cdot(H_2O)_n$ in fast processes having the rate constant of order 10^{-28} cm^6/s. This mechanism is supported by pressure dependent process (31) acting as a primary process. However, it must be noted that the rate constant for process (32) ($<5\times10^{-12}$ cm^3/cm at $T=343$ K), published by Viggiano et al. [21], is evidently smaller, therefore further experiments are required to resolve which of the three presented hypothesis on formation of OH^- and its clusters is valid.

The yield of $OH^-\cdot(H_2O)_n$ having $n<6$ is low while the yield of masses 125 ($OH^-\cdot(H_2O)_6$) and 143 ($OH^-\cdot(H_2O)_7$) is notably higher. Mass 125 has also been ascribed by Nagato et al. [11] to $NO_3^-\cdot HNO_3$. The low yields of clusters $OH^-\cdot(H_2O)_n$ having $n<6$ therefore suggests to us that the signal of mass 125 corresponds predominately to $NO_3^-\cdot HNO_3$ clusters and the contribution from $OH^-\cdot(H_2O)_6$ is only marginal. However, it should be noted that the ion with mass 125 is the most abundant negative ion in much of the terrestrial atmosphere. Similarly for mass 143 may be ascribed to $OH^-\cdot(HNO_3)_2$ or more probably the cluster $NO_3^-\cdot HNO_3\cdot H_2O$.

OH^- anions are not stable and undergo several ion–molecule reactions. The first one is very fast

$$OH^- + NO_2 \rightarrow NO_2^- + OH$$
$$k_{34} = 1\times10^{-9}\,\text{cm}^3/\text{s} \quad [7] \tag{34}$$

A second process is multi-step clustering with water molecules forming $OH^-\cdot(H_2O)_n$

$$OH^-\cdot(H_2O)_n + H_2O + M \rightarrow OH^-\cdot(H_2O)_{n+1} + M$$
$$n = 0, 1, 2\ldots \quad k_{35} \approx 5\times10^{-28}\,\text{cm}^6/\text{s} \quad [7] \tag{35}$$

Water clusters of OH^- can also react with NO_2

$$OH^-\cdot(H_2O)_n + NO_2^\bullet \rightarrow NO_2^-\cdot(H_2O)_{n-1} + OH + H_2O$$
$$n = 1, 2\ldots \quad k_{36} \approx 1.5\times10^{-11}\,\text{cm}^3/\text{s} \quad [7] \tag{36}$$

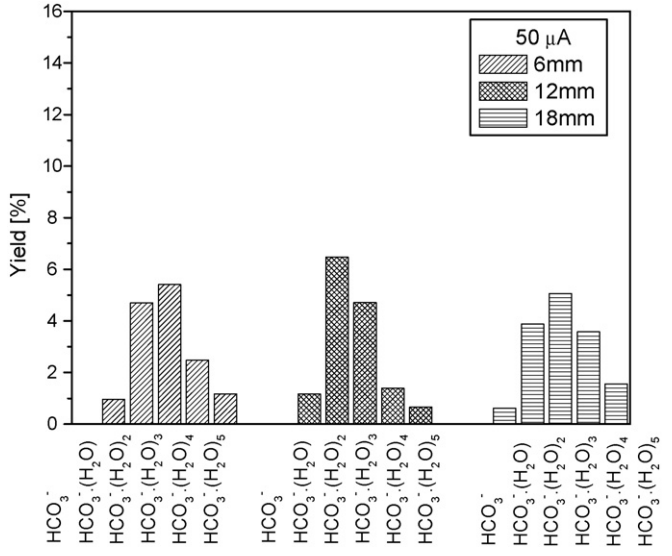

Fig. 12. The relative abundances of $HCO_3^-\cdot(H_2O)_n$ at three electrodes distances and the highest discharge current.

3.7. HCO_3^- ion and its clusters

Finally $HCO_3^-\cdot(H_2O)_n$ clusters were also detected (Fig. 12) and may be formed from HCO_3^- in the reactions

$$OH^-\cdot(H_2O)_n + CO_2^\bullet \rightarrow HCO_3^{-\bullet}(H_2O)_{n-1} + H_2O$$
$$n = 1, 2\ldots \quad k_{37} \approx 1.5\times10^{-11}\,\text{cm}^3/\text{s} \quad [7] \tag{37}$$

or by the three body process

$$OH^- + CO_2 + M \rightarrow HCO_3^- + M$$
$$k_{38} = 7.6\times10^{-28}\,\text{cm}^6/\text{s} \quad [11] \tag{38}$$

Once again we note the absence of any HCO_3^- parent ions in our spectra.

4. Conclusions

Mass spectra of negative ions obtained in an analysis of a negative corona discharge operating at atmospheric pressure and room temperature are very complex and have revealed many ionic species that have not been observed in previous studies. Neither of the parent negative ions O^- and O_2^- formed by dissociative and three body electron attachment processes were observed in the measured spectra. In contrast to previous experiments a relatively high abundance of $O_2^-\cdot(H_2O)_n$ clusters was observed, especially when the electrode separation was small. At larger separations $CO_3^-\cdot(H_2O)_n$, $O_3^-\cdot(H_2O)_n$, $NO_3^-\cdot(H_2O)_n$ and $HCO_3^-\cdot(H_2O)_n$ clusters were detected with yields of between 2 and 10% suggesting that in such reactors a rich and diverse chemistry is active in the discharge. Therefore further studies to explore this chemistry are urgently needed if we are to adopt atmospheric discharges for a variety of industrial and medical devices.

Acknowledgements

The authors are pleased to acknowledge the financial assistance of the Slovak Grant Agency VEGA under project 1/4017/07, the UK EPSRC research council (Grant GM/98944), the CEEPUS project A 103 and ESF projects EIPAM and COST.

References

[1] M.M. Shahin, Appl. Opt. 3 (1969) 106, Supplement on Electrophotography.
[2] P.S. Gardiner, J.D. Cragss, J. Phys. D: Appl. Phys. 10 (1977) 1003.
[3] J.D. Skalny, T. Mikoviny, S. Matejcik, N.J. Mason, Int. J. Mass Spectrom. 233 (2004) 317.
[4] C.A.M. de Vries, F.J. de Hoog, D.C. Schram, Proceedings of the 6th ISPC Montreal, 1983, p. 317.
[5] R. Peyrous, P. Coxon, J. Moruzzi, Proceedings of the 7th Int. Conf. on Gas Discharges and their Applications, London, 1982, p. 169.
[6] A. Luts, J. Geophys. Res. 100 (1995) 1487.
[7] B. Gravendeel, F.J. de Hoog, J. Phys. B: At. Mol. Phys. 20 (1987) 6337.
[8] S.J. Ross, A.J. Bell, Int. J. Mass Spectrom. 218 (2002) L1.
[9] J.D. Skalny, G. Horvath, N.J. Mason, J. Optoelect. Adv. Mat. 9 (2007) 887.
[10] K. Nagato, C.S. Kim, M. Adachi, K. Okuyama, Aerosol Sci. 36 (2005) 1036.
[11] K. Nagato, Y. Matsui, T. Miyata, T. Yamamuchi, Int. J. Mass Spectrom. 248 (2006) 142.

[12] W.L. Lama, C.F. Gallo, J. Appl. Phys. 45 (1974) 103.
[13] B. Elliason, Electrical Discharge in Oxygen Part 1: Basic data, Rate coefficients and Cross Sections, Report KLR 83/40 C, Brown Boveri Forschungszentrum, Baden-Dättwil, 1985.
[14] H. Hokazono, M. Obara, K. Midorikawa, H. Tashiro, J. Appl. Phys. 69 (1991) 6850.
[15] S. Sakata, T. Okada, J. Aerosol Sci. 25 (1994) 879.
[16] J.O. Ballenthin, W.F. Thorn, T.M. Miller, A.A. Viggiano, D.E. Hunton, M. Koike, Y. Kondo, N. Takegawa, H. Irie, H. Ikeda, J. Geophys. Res. 108 (2003) ACH7.
[17] F. Arnold, J. Scheid, T. Stilp, H. Schlager, M.E. Reinhardt, Geophys. Res. Lett. 12 (1992) 2421.
[18] S.T. Arnold, R.A. Morris, A.A. Viggiano, J. Chem. Phys. 103 (1995) 2454.
[19] A.A. Viggiano, F. Arnold, Planet. Space. Sci. 31 (1983) 813.
[20] D.L. Albritton, Atomic Data Nucl. Tables 22 (1978) 1.
[21] A:A. Viggiano, R.A. Morris, C.A. Deakyne, F. Dale, J.F. Paulson, J. Phys. Chem. 94 (1990) 8193.